Optical coherence tomography in dermatology: a review

Julia Welzel

Angaben zur Veröffentlichung / Publication details:

Welzel, Julia. 2001. "Optical coherence tomography in dermatology: a review." *Skin Research and Technology* 7 (1): 1–9. https://doi.org/10.1034/j.1600-0846.2001.007001001.x.

Optical coherence tomography in dermatology: a review

Julia Welzel

Department of Dermatology, Medical University of Lübeck, Lübeck, Germany

Background/aims: Optical coherence tomography (OCT) is a non-invasive technique for morphological investigation of tissue. Since its development in the late 1980s it is mainly used as a diagnostic tool in ophthalmology. For examination of a highly scattering tissue like the skin, it was necessary to modify the method. Early studies on the value of OCT for skin diagnosis gave promising results.

Methods: The OCT technique is based on the principle of Michelson interferometry. The light sources used for OCT are low coherent superluminescent diodes operating at a wavelength of about 1300 nm. OCT provides two-dimensional images with a scan length of a few millimeters (mm), a resolution of about 15 μm and a maximum detection depth of 1.5 mm. The image acquisition can be performed nearly in real time. The measurement is non-invasive and with no side effects.

Results: The in vivo OCT images of human skin show a strong scattering from tissue with a few layers and some optical inhomogeneities. The resolution enables the visualization of architectural changes, but not of single cells. In palmoplantar skin, the thick stratum corneum is visible as a low-scattering superficial well defined layer with spiral sweat gland ducts inside. The epidermis can be distinguished from the dermis. Adnexal structures and blood vessels are low-scattering regions in the upper dermis. Skin tumors show a homogenous signal distribution. In some cases, tumor borders to healthy skin are detectable. Inflammatory skin diseases lead to changes of the OCT image, such as thickening of the epidermis and reduction of the light attenuation in the dermis. A quantification of treatment effects, such as swelling of the horny layer due to application of a moisturizer, is possible. Repeated measurements allow a monitoring of the changes over time.

Conclusion: OCT is a promising new bioengineering method for investigation of skin morphology. In some cases it may be useful for diagnosis of skin diseases. Because of its non-invasive character, the technique allows monitoring of inflammatory diseases over time. An objective quantification of the efficacy and tolerance of topical treatment is also possible. Due to the high resolution and simple application, OCT is an interesting addition to other morphological techniques in dermatology.

Key words: optical coherence tomography (OCT) – in vivo investigation – bioengineering method – skin diseases

In dermatology , most skin diseases can be diagnosed by the naked eye. For investigation of cellular changes, conventional excisional biopsy is still the gold standard. Because biopsies are invasive and may cause side effects that make follow-up studies difficult, the development of non-invasive morphological techniques was pushed along. High-frequency sonography has become established in dermatology, but the resolution and contrast of the ultrasound images have not come up to expectations (1). Among others, high resolution optical techniques that cause no side effects when using visible or infrared light are being developed.

Optical coherence tomography (OCT) is based on the more than 100-year-old principle of Michelson interferometry. The technique was first introduced by Fercher et al. (2) and Huang et al. (3) for investigation of the human eye. It has proved to be of value for visualization of changes in the retina and the cornea (4–7). Some experimental studies on other organs revealed the value of this new optical technique (8–13). In contrast to the eye, which is naturally a low light scattering transparent medium, skin is nearly non-transparent. The lack of transparency is due to absorption and scattering; the first is mainly influenced by the concentration of melanin and haemoglobin, the latter by differences in the refraction index. In the wavelength range of 700 to 1300 nm, the so-called diagnostic window, absorption is relatively low, so that light penetrates deep into the skin and optical inhomogeneities are the main factor influencing the image. When illuminating the skin, most of the photons are scattered more than once. This leads to artifacts when detecting all the backscattered photons for image information, because they are dislocated in space and time. Only a small part of the photons directly reflected from a structure carry real image information. The problem with OCT is to distinguish this small fraction from the intense background noise; solving the problem involves looking for interference

between the sample and the reference beam and using the high output power and dynamic range of the system. Some experimental OCT systems have already been used in dermatology (14, 15). Early in vivo OCT images of the human skin gave promising results (16–21).

OCT Technique

For OCT, light sources with wavelengths in the near infrared, most of them operating at 1300 nm, are used. The light sources are superluminescent diodes with a short coherence length of about 15 µm. Alternatively, a laser can be used, in which the short coherence length is achieved by ultrashort femtosecond pulses. The light is coupled to a single-mode fiberoptic interferometer and divided into a reference beam and a probe beam. The reference signal is reflected from a scanning mirror system. The light in the sample arm is focused onto the superficial skin layers, backscattered and recombined again with the reflected reference signal (Fig. 1). Interference occurs only if the path length of both beams match to within the short coherence length of the light source. The interference signal gives, therefore, information about the path length distribution of the sample beam due to optical inhomogeneities of the tissue. By lateral scanning, OCT provides two-dimensional cross-sectional images of the skin. The axial resolution depends on the coherence length of the light source, whereas the lateral resolution is given by the focal spot size and the scan step. Both values are about 15 µm for conventional OCT systems. The detection depth depends on the wavelength, the scattering and the attenuation of the light inside the tissue and varies from 1 to 1.5 mm in skin. By applying a scan frequency of 100 Hz, the time for one image of 4 mm scan length is about 4 s. Therefore, real-time imaging is almost reached, and artifacts due to slight movements of the skin do not play an important role. The scans are represented in logarithmic false color or grey scale images.

A calculation of the thickness of layers, the intensity of the signal and the light attenuation coefficient in different depths can be performed on the averaged A-scan in a region of interest in the OCT image (Fig. 2). These parameters are useful for quantification of changes. Because light propagation in tissue differs from that in air due to differences in refraction, the dimensions must be corrected by dividing by the refractive index of skin, which is about 1.4 (22).

The OCT measurement is unobtrusive and safe. It is not noticeable by the subject and has no side effects. Because of the fast scanning mode and the low output power of the light source (in a range of a few milliwatts), the technique meets the safety standards for irradiation of tissue. Our OCT studies were approved by the local ethics committee.

For the special demands of practical dermatological operation, a compact OCT system with a flexible applicator was constructed at the Medical Laser Center Lübeck, Germany; the system will be commercially available (Fig. 3). This prototype was used for systematic studies on various skin changes in healthy volunteers and patients.

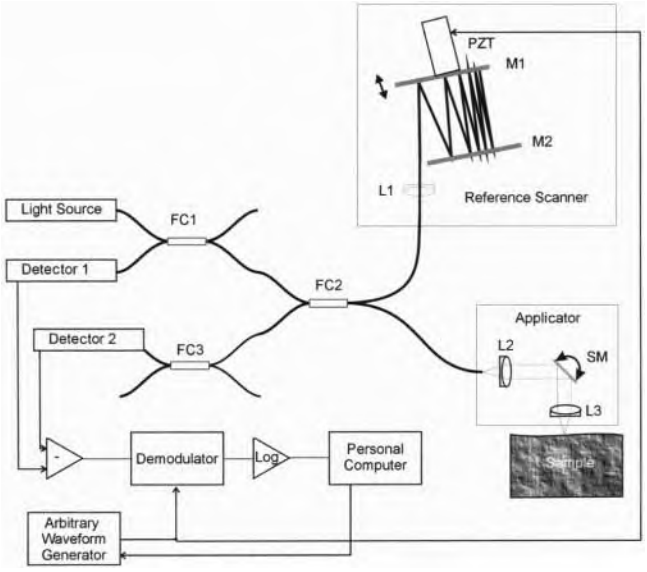

Fig. 1. OCT system for dermatology. The light from the superluminescent diode is coupled into optical fibers and divided into a reference and a sample beam. The reference beam is reflected by a scanning mirror system, and the probe beam is focused onto the skin. The backscattered photons are recombined again with the reference signal and are detected by interference if they match to within the short coherence length.

OCT of Healthy Skin

The reflectivity of skin leads to a signal intensity peak on the surface. Below this entrance signal, several

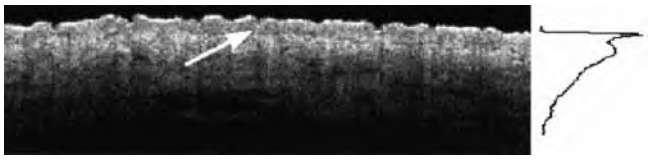

Fig. 2. OCT image of healthy skin of the forearm. On the right side, the averaged A-scan is represented. The thickness of the epidermis is 195 µm; the relationship between the entrance signal and the second intensity peak on the border to the dermis is 1.7; the light attenuation coefficient in the upper dermis is 1.8/mm. (830 nm OCT, 4 mm×1.3 mm)

Fig. 3. The OCT system and the hand piece in front of the keyboard.

layers and structures can be distinguished in the OCT image.

The stratum corneum is only visible on palmoplantar skin. At this location it is a thick, homogenous, low-scattering, well defined superficial layer with some spiral, strong scattering sweat gland ducts inside (Fig. 4).

At other locations, the epidermis is the first layer. It shows less intense signals than the dermis and can be distinguished from the upper corium if the border is flat and not too toothed. In the averaged A-scan, the border to the dermis is characterized by a second intensity peak (Fig. 2).

The dermis shows intense signals with some lower reflecting regions, corresponding to hair follicles and sebaceous glands (Fig. 5). Hairs on the skin surface cause signal shadows. The blood vessels appear as signal-free round or longish structures. If the dermis is thin, the low reflecting subcutis is visible in the lower parts of the image.

A comparison between corresponding histological sections and the investigation of defined bullous diseases allow assignment of the different layers seen in OCT images (Fig. 6a & b).

The reflection of the skin surface can be reduced by application of an ointment or glycerol (Fig. 7a & b). The topical treatment makes the skin more transparent, reduces light scattering and, therefore, increases detection depth. Vargas et al. (23) investigated the influence of glycerol on the light scattering properties of skin. They found a reduction in the lack of

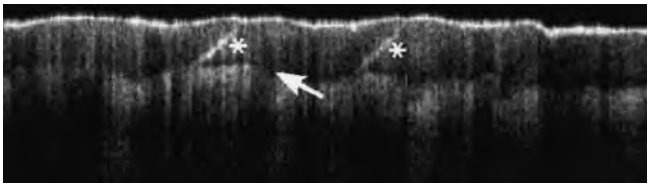

Fig. 4. In vivo OCT image of healthy skin of the finger tip. The first layer is the thick stratum corneum with spiral sweat gland ducts (stars). The stratum granulosum is marked by an arrow. (4 mm×1.1 mm)

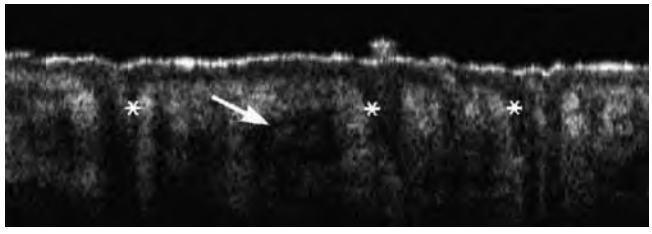

Fig. 5. Healthy skin of the cheek shows a less signal-intense epidermis as the first superficial layer below the entrance signal, some hair follicles (stars) and sebaceous glands (arrow). (4 mm×1.4 mm)

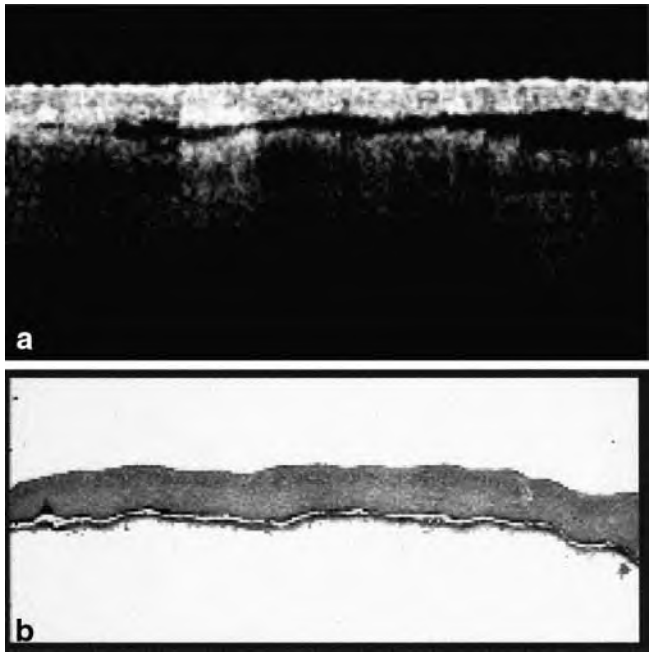

Fig. 6. OCT image (a) and corresponding histological section (b) of an intraepidermal, mechanically induced blister on the thumb. The cleft location is the stratum granulosum. (830 nm OCT, 2 mm×1.1 mm; histology H-E, ×50)

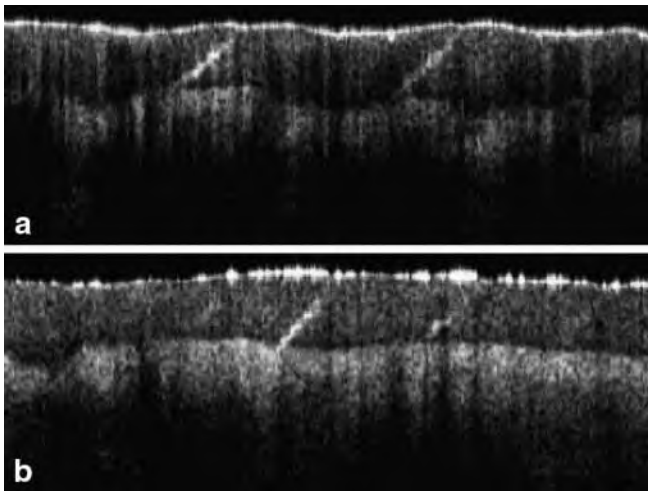

Fig. 7. Healthy skin of the finger tip before (a) and directly after application of glycerol (b). The treatment leads to an increase in the detection depth and to an attenuation of the entrance signal. (4 mm×1.1 mm)

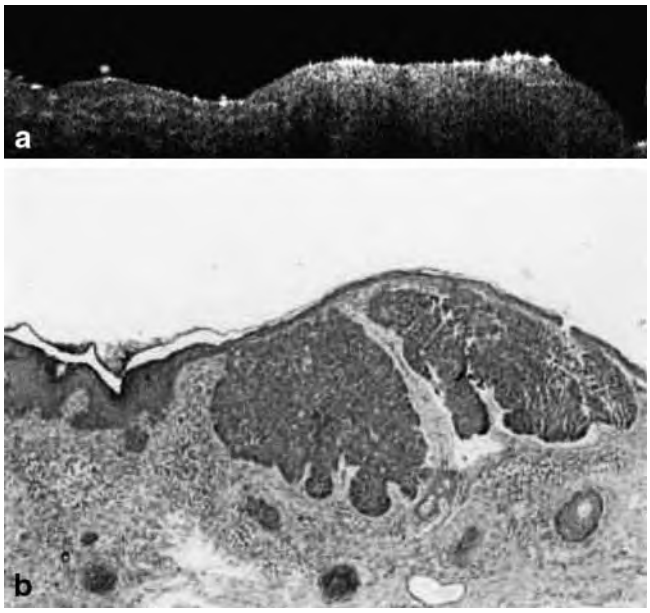

Fig. 8. OCT (a) and corresponding histology (b) of a basal cell carcinoma on the lower eyelid. The signal distribution in the tumor is more homogenous compared to healthy skin. (OCT 6 mm×1.5 mm; histology H-E, ×50)

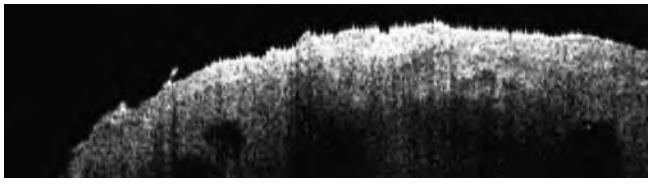

Fig. 9. Cystic basal cell carcinoma on the lower eyelid. The cysts are represented as signal-free cavities. (OCT 4 mm×1.1 mm)

transparency after a dermal injection of glycerol. This effect was explained by the hyperosmolarity of the substance causing a water shift from intracellular to extracellular space, which leads to a matching of the refractive indices of the collagen and the ground substance. The effect of glycerol on the stratum corneum is different. The substance is a potent natural moisturizing factor and increases the water binding capacity of the horny layer. Our comparative studies on the effect of topical treatment on OCT images have shown that all products induce an immediate reduction of the light attenuation and an increase of the detection depth of the light signal. The products act like an immersion oil and reduce the opacity of the stratum corneum.

OCT of Skin Tumors

In OCT images of epithelial skin tumors, the derivation of tumor cell aggregates from the epidermis is visible. Solid tumors show a homogenous signal distribution (Fig. 8a & b). Cystic structures are identifiable by signal-free areas (Fig. 9). In some cases, the lateral border of the tumor adjacent to healthy skin is detectable. In basal cell carcinomas, the tumor cell aggregates can be distinguished from the fibrous stroma.

Melanocytic skin tumors show a higher light scattering and – like other tumors – show a more homogenous signal distribution compared with healthy skin. The second intensity peak, representing an intact border between epidermis and dermis, disappears in infiltrative growing malignant melanoma (Fig. 10a & b). A differential diagnosis between benign nevi and malignant melanomas is not possible using OCT because the resolution is not high enough to show single cells. The infiltration depth of melanomas can be measured only in thin tumors up to 1 mm in tumor thickness because of the limitation of the light penetration depth into the skin.

Some skin tumors show a characteristic pattern. Seborrheic keratoses are inhomogeneous with areas of poor and strong signals sharply demarcated from the dermis (Fig. 11). Hemangiomas show several signal-poor cavities in the dermis without affecting the epidermis (Fig. 12).

OCT of Inflammatory Skin Diseases

Changes due to inflammation are clearly visible in OCT images. A parakeratotic stratum corneum appears as a multilayered thickened entrance signal. A

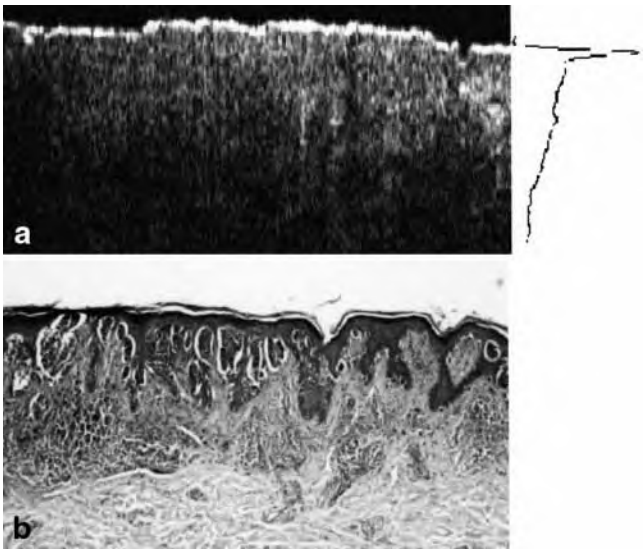

Fig. 10. OCT (a) and histology (b) of a malignant melanoma. On the averaged A-scan (right), no second intensity peak at the level of the basal membrane is detectable. (OCT 4 mm×1.8 mm; histology H-E, ×50)

Fig. 11. A seborrheic keratosis shows irregular signal-rich and signal-poor areas corresponding to the horny cysts. The border between the tumor and the dermis is sharply demarcated (arrow). (4 mm×1.1 mm)

Fig. 12. The blood vessels in a hemangioma are represented as signal-free cavities in the upper dermis. The intact epidermis is elevated above the tumor. (4 mm×1.1 mm)

distance measurement between the entrance peak and the second intensity peak in the averaged A-scan gives information on the epidermal thickness. Therefore, acanthosis of the epidermis due to proliferation or spongiosis can be observed and quantified over time. An inflammatory reaction of the skin is accompanied by edema, leading to a reduction of the light attenuation coefficient in the dermis. The dilation of blood vessels in the upper dermis is also visible.

OCT of psoriatic skin shows a strong entrance signal, composed of several parallel layers (Fig. 13).

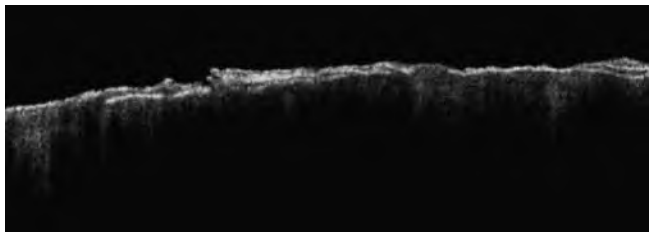

Fig. 13. Psoriasis with severe hyperkeratosis. The thickened stratum corneum is represented by parallel multilayered lines. (4 mm×1.8 mm)

Scales may cause signal shadows due to the total reflection of the light from the surface. Pustules are seen as intraepithelial holes with strongly scattering, signal-intense structures inside (Fig. 14). The acanthosis of epidermis can be quantified and monitored over time and under treatment. In psoriatic skin, the second intensity peak is lower than in healthy adjacent skin. This is due to the toothed border between epidermis and dermis with pronounced rete-ridges in psoriasis. Therefore, the border is not a well defined flat line when averaging the A-scan signals. In the dermis, light scattering is changed because of the inflammation. Dilated blood vessels are visible in the OCT image (Fig. 15a & b).

In eczematous skin, the surface shows more folds. As in psoriasis, the entrance signal is pronounced and thicker due to the parakeratosis. The acanthosis of the epidermis as well as the dilation of blood vessels in the upper dermis is visible in the OCT image. The edema leads to a decrease of the light scattering in the dermis (Fig. 16).

Blisters appear in OCT as signal-free cavities. Intraepidermal blisters can be distinguished from subepidermal blisters by looking for the location of the cleft at the lateral border of the blister. A phototoxic contact dermatitis shows multilocular blisters in the lower epidermis. In herpes zoster, the cavity is a confluence of intraepidermal blisters with remnants of clotted large acantholytic keratinocytes inside. In pemphigus vulgaris, the roof of the blister is very thin

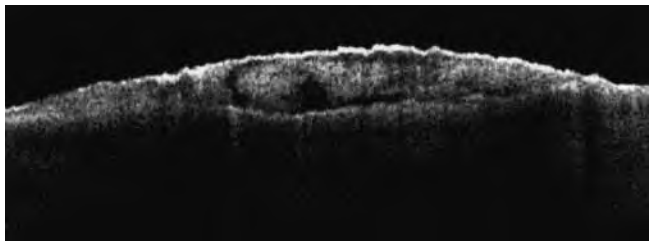

Fig. 14. A psoriatic pustule appears as an intraepidermal cavity filled with inhomogeneous signal strong material. (4 mm×1.8 mm)

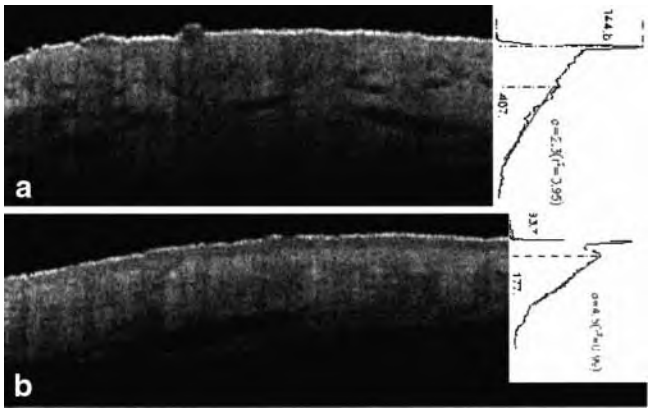

Fig. 15. Psoriasis (a) and healthy adjacent skin (b) of the same subject. The averaged A-scans are shown on the right. In psoriasis, the epidermis is thickened, and the second intensity peak and the light attenuation coefficient in the dermis are lower compared to healthy skin.

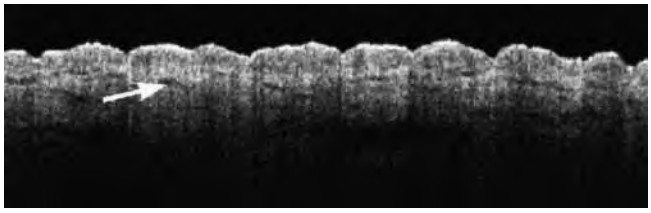

Fig. 16. Irritant contact dermatitis 4 days after application of 5% sodium lauryl sulfate on the forearm. Compared to healthy skin of the same subject (see Fig. 2), the contact dermatitis shows larger folds on the surface, a pronounced entrance signal, a thickened epidermis and dilated blood vessels (arrow) in the dermis. (830 nm OCT, 4 mm×1.8 mm)

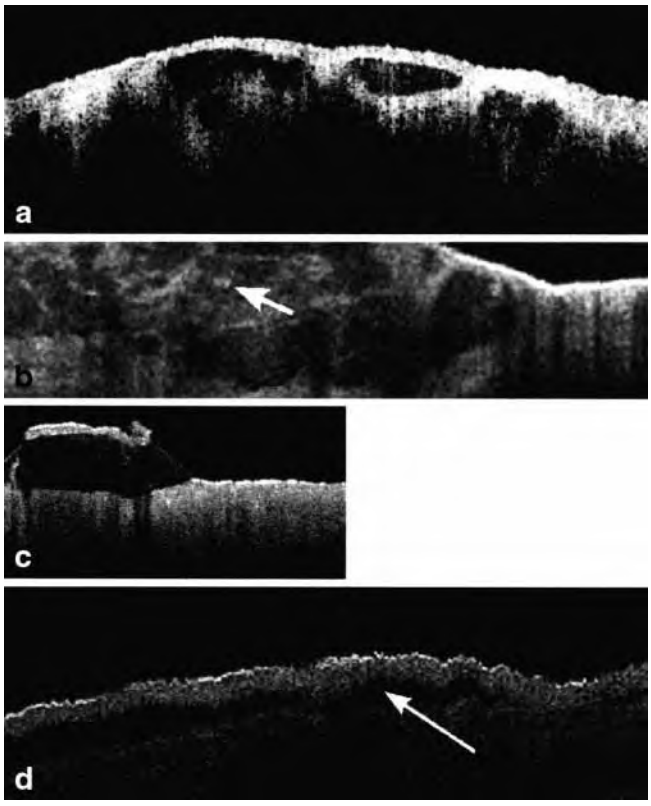

Fig. 17. a) Phototoxic contact dermatitis with intraepidermal multilocular blisters (830 nm OCT, 4 mm×1.4 mm). b) Herpes zoster with a confluent intraepidermal blister with remnants of acantholytic keratinocytes (arrow) (4 mm×1.1 mm). c) Pemphigus vulgaris with a large intraepidermal bulla. The roof is very thin (830 nm OCT, 2 mm×0.8 mm). d) Bullous pemphigoid with a subepidermal blister. The whole epidermis is elevated. The cleft (arrow) is between the epidermis and the dermis. (4 mm×1.8 mm)

compared to the bulla in bullous pemphigoid, where the whole epidermis is elevated (Fig. 17a–d).

Some skin diseases can be easily diagnosed using OCT. The characteristic chimney-like hyperkeratosis in porokeratosis is visible in the OCT image as well as the mite in scabies (Figs. 18 & 19).

Fig. 18. Actinic porokeratosis shows the characteristic chimney-like hyperkeratotic column in the center of the OCT image. (4 mm×1.1 mm)

OCT for Evaluation of Treatment Effects

Topical treatment influences the optical appearance of skin in OCT. Directly after application, ointments are visible on the skin surface as a strongly scattering layer. After some minutes the penetration of the product into the stratum corneum can be observed (Fig. 20a–d). Hydrating effects of moisturizers on the stratum corneum as well as epidermal atrophy after steroid therapy can be quantified by thickness measurements. Furthermore, OCT allows non-invasive monitoring of the healing of inflammatory skin diseases under treatment. Occlusive or prolonged contact of healthy skin with water or soaps leads to a swelling of the horny layer. In the OCT images, the stratum corneum is thickened and shows stronger light scattering than before treatment (Fig. 21a & b). Obviously, the water content and the shape of the corneocytes influence the optical properties. All these changes can be quantified by measurements of distances between peaks, signal intensities and light attenuation coefficients in different depths of the skin on the averaged A-scan.

Conclusion

OCT is a new morphological method for non-invasive in vivo investigation of the skin. It provides two-dimensional images of a lateral dimension up to 10 mm, a detection depth of about 1.5 mm and an axial and lateral resolution of about 15 µm. With these parameters, the stratum corneum, the epidermis and the upper dermis can be investigated, as well as skin appendages and blood vessels. The resolution is not high enough to show single cells, but the architecture of a lesion can be assessed. The measurement has no side effects and can be performed nearly in real time. The use of optical fibers allows even hardly accessible regions of the skin to be reached. Furthermore, OCT is a fast, simple, compact and relatively inexpensive technique.

The clinical studies of OCT in dermatology revealed that the method is of value for diagnosis of some inflammatory and bullous skin diseases and for differential diagnosis of some tumors – for example, between solid and cystic lesions. The resolution is not sufficient for judging the grade of melanocytic tumors. The use of OCT for non-invasive monitoring of inflammatory skin diseases is of special interest (24). OCT allows an objective, high-resolution quantification of the degree of acanthosis and edema over time and under different therapeutic regimes. Therefore, OCT can also be used for evaluation of the efficacy and tolerance of topical treatment.

Compared to other non-invasive bioengineering methods, OCT has some advantages. Due to the higher resolution, the OCT images give more details and contrast than high resolution ultrasound (Fig. 22). Compared to confocal scanning laser microscopy (25, 26), which provides a higher resolution, the detection

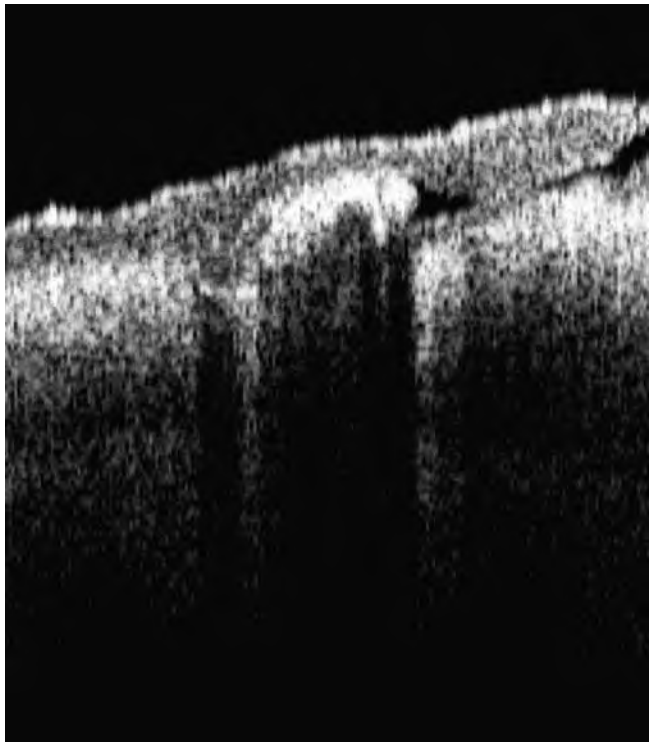

Fig. 19. OCT of a scabies mite in the center with a burrow behind. (1 mm×1.2 mm)

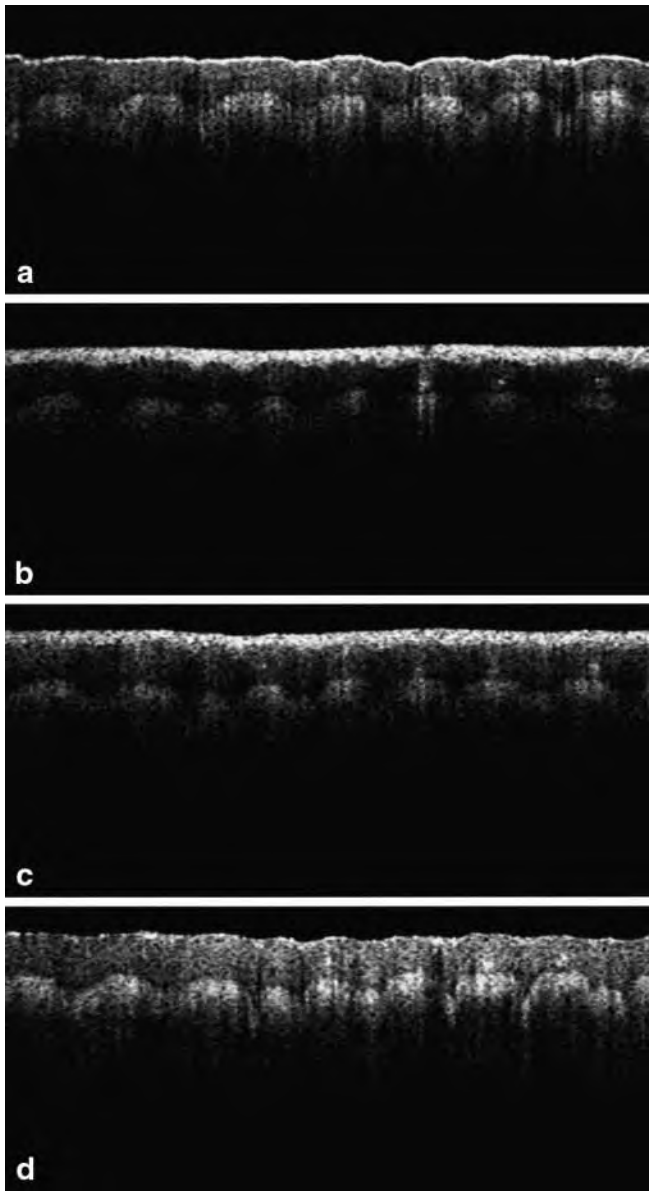

Fig. 20. Healthy skin on the thumb before (a), directly after application of an ointment containing 10% urea (b), after 35 min (c) and after wiping off the cream (d). The ointment is visible as a strongly scattering layer on the skin surface. After a time, the penetration into the stratum corneum can be observed. Compared to (a), the stratum corneum is thickened in (d) due to increased water content. (4 mm×1.8 mm)

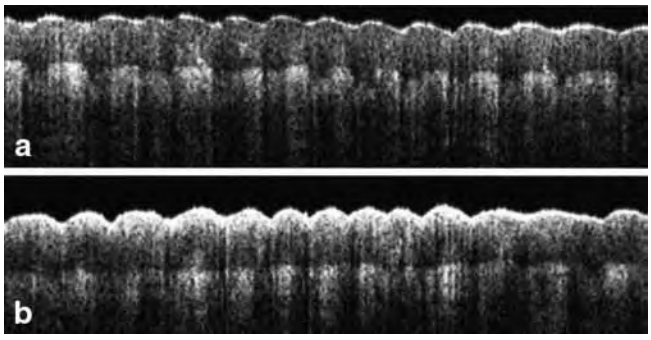

Fig. 21. Healthy skin on the fingertip before (a) and after 15 min bath in a solution of a synthetic detergent (b). After treatment, the stratum corneum shows swelling and stronger light scattering. (4 mm×1.1 mm)

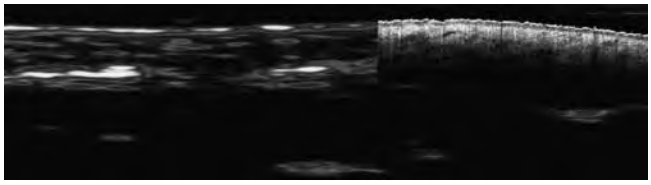

Fig. 22. 20 MHz ultrasound and OCT of the same region on the forearm. The dimensions are equal. Compared to ultrasound, the OCT image has a lower detection depth, but a much higher resolution, which allows differentiation of the epidermis and small blood vessels in the dermis. (Ultrasound 12 mm×3.5 mm; OCT 5 mm×1.3 mm)

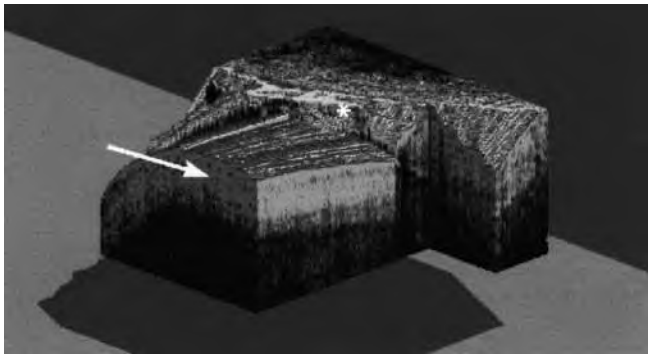

Fig. 23. In vivo three-dimensional OCT of the nail plate (arrow) of a finger. The proximal nail fold and the cuticle are marked by a star. A section is taken out of the image to allow a view into the matrix region. (4.2 mm×4 mm×1.4 mm)

depth and the image size of OCT is much greater. Furthermore, the technique is much simpler than magnetic resonance imaging of the skin (27, 28).

Future Developments

The fast scanning mode of OCT allows continuous measurements of a dynamic process over several minutes and a display of the changes as a movie. This possibility has already been used in ophthalmology to demonstrate the light reaction of the iris and in dermatology to show the swelling of the stratum corneum after treatment with urea. By fast scanning of parallel two-dimensional OCT images, a three-dimensional image of a structure can be calculated and displayed (Fig. 23) (29).

As in ultrasound, the Doppler effect can be used to visualize and quantify blood flow (30). Such a color duplex OCT is already realized for investigation of the blood vessels of the human retina.

The image information of OCT depends on the wavelength of the light source because the degree of absorption of water, hemoglobin and melanin depends on the wavelength. This effect can be used for quantification of the water content of the epidermis and dermis if two different wavelengths are used simultaneously for image acquisition and the images are compared with respect to the light attenuation coefficient.

Higher output power of the light source enhances the detection depth, and shorter coherence length enhances the axial resolution. Therefore, the development of new light sources for OCT will give further perspectives on the clinical value of this method as a diagnostic tool in dermatology. The experimental application of a short-pulsed femtosecond laser has demonstrated that a resolution of 3 to 5 µm can be reached, which will allow the detection of single cells (31).

In summary, OCT at its present technical realization is a valuable non-invasive morphological method that is starting to become commercially available. Further developments will expand the possibilities and indications of OCT for practical use in dermatology.

Acknowledgements

I would like to thank Prof. Dr. R. Birngruber, Dipl.-Phys. R. Engelhardt, Dipl.-Phys. E. Lankenau, Dr. J. Noack and Dipl.-Ing. C. Scholz from the OCT group of the Medical Laser Center Lübeck GmbH for excellent technical and scientific support. This work was partly supported by the German Ministry of Science and Research (BMBF), FK Nr. 13N7151-6.

References

1. El-Gammal S, Auer T, Hoffmann K, Altmeyer P, Paßmann C, Ermert H. High-resolution ultrasound of the human epidermis. In: Serup J, Jemec GBE, eds. Handbook of non-invasive methods and the skin. Boca Raton, Ann Arbor, London, Tokyo: CRC Press, 1995: 125–131.
2. Fercher AF, Mengedoht K, Werner W. Eye length measure-

ment by interferometry with partially coherent light. Opt Lett 1988: 13: 186–188.
3. Huang D, Swanson EA, Lin CP, et al. Optical coherence tomography. Science 1991: 254: 1178–1181.
4. Hee MR, Izatt JA, Swanson EA, et al. Optical coherence tomography of the human retina. Arch Ophthalmol 1995: 113: 325–332.
5. Hee MR, Puliafito CA, Wong C, et al. Optical coherence tomography of macular holes. Ophthalmology 1995: 102: 748–756.
6. Hee MR, Puliafito CA, Wong C, et al. Optical coherence tomography of central serous chorioretinopathy. Am J Ophthalmol 1995: 120: 65–74.
7. Shuman JS, Hee MR, Puliafito CA, et al. Quantification of nerve fiber layer thickness in normal and glaucomatous eyes using optical coherence tomography. Arch Ophthalmol 1995: 113: 586–596.
8. Boppart SA, Brezinski ME, Pitris C, Fujimoto JG. Optical coherence tomography for neurosurgical imaging of human intracortical melanoma. Neurosurgery 1998: 43: 834–841.
9. Brezinski ME, Tearney GJ, Bouma B, et al. Optical biopsy with optical coherence tomography. Ann N Y Acad Sci 1998: 838: 68–74.
10. Brezinski ME, Tearney GJ, Bouma BE, et al. Imaging of coronary artery microstructure (in vitro) with optical coherence tomography. Am J Cardiol 1996: 77: 92–93.
11. Herrmann JM, Pitris C, Bouma BE, et al. High-resolution imaging of normal and osteoarthritic cartilage with optical coherence tomography. J Rheumatol 1999: 26: 627–635.
12. Pitris C, Goodman A, Boppart SA, Libus JJ, Fujimoto JG, Brezinsiki ME. High-resolution imaging of gynecologic neoplasms using optical coherence tomography. Obstet Gynecol 1999: 93: 135–139.
13. Tearney GJ, Brezinski ME, Southern JF, Bouma BE, Boppart SA, Fujimoto JG. Optical biopsy in human pancreatobiliary tissue using optical coherence tomography. Dig Dis Sci 1998: 43: 1193–1199.
14. Pan Y, Lankenau E, Welzel J, Birngruber R, Engelhardt R. Optical coherence gated imaging of biological tissues. IEEE J Selected Top Quantum Electronics Lasers Med Biol 1996: 2: 1029–1034.
15. Schmitt JM, Yadlowski MJ, Bonner RF. Subsurface imaging of living skin with optical coherence microscopy. Dermatology 1995: 191: 93–98.
16. Gladkova ND, Petrova GA, Nikulin NK, et al. In vivo optical coherence tomography imaging of human skin: norm and pathology. Skin Res Technol 2000: 6: 6–16.
17. Pagnoni A, Knüttel A, Welker P, et al. Optical coherence tomography in dermatology. Skin Res Technol 1999: 5: 83–87.
18. Welzel J, Lankenau E, Birngruber R, Engelhardt R. Optical coherence tomography of the human skin. J Am Acad Dermatol 1997: 37: 958–963.
19. Welzel J, Lankenau E, Pan Y, Birngruber R, Engelhardt R. Optical coherence tomography of the skin. In: Elsner P, Barel AO, Berardesca E, Gabard B, Serup J, eds. Skin bioengineering. Techniques and applications in dermatology and cosmetology. Curr Probl Dermatol. Basel: Karger, 1998: 26: 27–37.
20. Welzel J, Lankenau E, Engelhardt R. Optische Kohärenztomographie als ein neues Verfahren zur nicht-invasiven Darstellung oberflächennaher Strukturen der Haut. In: Garbe C, Rassner G, eds. Dermatologie – Leitlinien und Qualitätssicherung für Diagnostik und Therapie. Berlin, Heidelberg, New York: Springer, 1998: 9–12.
21. Welzel J. Optische Kohärenztomographie – ein neues nichtinvasives Verfahren zur morphologischen Darstellung der Haut. Akt Dermatol 2000: 26: 174–177.
22. Tearney GJ, Brezinski ME, Southern JF, Bouma BE, Hee MR, Fujimoto JG. Determination of the refractive index of highly scattering tissue by optical coherence tomography. Opt Lett 1995: 20: 2258–2261.
23. Vargas G, Chan EK, Barton JK, Rylander HG, Welch AJ. Use of an agent to reduce scattering in skin. Lasers Surg Med 1999: 24: 133–141.
24. Welzel J, Bruhns M, Schröder C, Birngruber R. Clinical optical coherence tomography studies in dermatology: inflammatory skin diseases and treatment effects. In: Biomedical optics: new concepts in therapeutic laser applications, novel biomedical optical spectroscopy, imaging and diagnostics, advances in optical imaging, photon migration, and tissue optics. OSA Technical Digest (Optical Society of America, Washington, DC), 1999: 366–368.
25. Corcuff P, Hadjur C, Chaussepied C, Toledo-Crow R. Confocal laser microscopy of the in vivo human skin revisited. In: Proceedings of three-dimensional and multidimensional microscopy: image acquisition and processing VI. Soc Photo-Opt Instr Eng 1999: 3605: 73–81.
26. Veiro JA, Cummings PG. Imaging of skin epidermis from various origins using confocal laser scanning microscopy. Dermatology 1994: 189: 16–22.
27. El Gammal S, Hartwig R, Aygen S, Bauermann T, el Gammal C, Altmeyer P. Improved resolution of magnetic resonance microscopy in examination of skin tumors. J Invest Dermatol 1996: 106: 1287–1292.
28. Song HK, Wehrli FW, Ma J. In vivo MR microscopy of human skin. Magn Reson Med 1997: 37: 185–191.
29. Boppart SA, Bouma BE, Pitris C, et al. Intraoperative assessment of microsurgery with three-dimensional optical coherence tomography. Radiology 1998: 208: 81–86.
30. Chen Z, Milner TE, Wang X, Srinivas S, Nelson JS. Optical Doppler tomography: imaging in vivo blood flow dynamics following pharmacological intervention and photodynamic therapy. Photochem Photobiol 1998: 67: 56–60.
31. Fujimoto JG, Bouma B, Tearney GJ, et al. New technology for high-speed and high-resolution optical coherence tomography. Ann N Y Acad Sci 1998: 838: 95–107.

Address:
Julia Welzel
Klinik für Dermatologie und Venerologie
Universitätsklinikum Lübeck
Ratzeburger Allee 160
D-23538 Lübeck
Germany

Tel: +49 451 500 2515
Fax: +49 451 500 2981
e-mail: welzel@medinf.mu-luebeck.de